International Forum on Aeroelasticity and Structural Dynamics
IFASD 2017
25-28 June 2017 Como, Italy

MODAL FORMULATION FOR GEOMETRICALLY NONLINEAR STRUCTURAL DYNAMICS

Renato R. Medeiros[1], Carlos E. S. Cesnik[1], and Etienne B. Coetzee[2]

[1]Department of Aerospace Engineering
University of Michigan
1320 Beal Ave, Ann Arbor, MI 48109 USA
renatorm@umich.edu
cesnik@umich.edu

[2]Airbus Operations
Pegasus House, Aerospace Avenue, Filton, Bristol BS99 7AR, United Kingdom
etienne.coetzee@airbus.com

Keywords: Reduced Order Modeling, very flexible aircraft, nonlinear modal analysis

Abstract: This paper describes a general formulation for the solution of geometrically nonlinear structural problems with Reduced Order Models. Based on the Euler-Lagrange equations, the approach allows any choice of degrees of freedom and fitting functions for the potential energy and displacements. It is particularly suitable to the modeling of cantilevered structures, since it includes the nonlinear displacements into the kinetic energy, correcting inertia terms which used to be neglected in previous developments. The dynamic analyses of a beam and a wing box undergoing large displacements in the time-domain illustrate the method.

1 INTRODUCTION

Modal analysis has been the standard in aeroelastic tools used in industry. However, the increasing flexibility of commercial aircraft and the recent designs of very flexible Unmanned Aerial Vehicles (UAV's) pose a challenge to that approach. From the structural point of view, large deformations change the stiffness and the mass matrices in such a way that displacements can no longer be represented by the standard linear modal approach. Currently, time-domain solutions obtained with either nonlinear beam-based formulations (e.g., University of Michigan's NAST solver [1]) or full nonlinear FEM (e.g., AERO [2]) are used for the coupled aeroelastic/flight dynamics analysis when geometric nonlinearities are considered. While beam modeling may not be sufficient to capture complex structural details present in aircraft wings, detailed FEM may be very costly for dynamic simulations.

The goal of this paper is to present a framework for nonlinear structural modal-based methods that captures the geometric nonlinear effects which arise in the regime of large deformations of airplanes with high-aspect-ratio wings. It builds on previous work of nonlinear stiffness methods and extends the problem to account for the impact of large deflections on the modal mass. The modified modal methods include stiffness nonlinear terms that depend on the generalized coordinates. The structural deformation is calculated not only by normal modes but also by higher-order modal components that account for the foreshortening effect at high-aspect-ratio wing structures.

Nonlinear structural reduced order models (ROMs) have been developed since the 70s, but most of the progress happened only after Muravyov *et al.* [3] proposed to use results from nonlinear static analysis to build surrogate models satisfying the structural dynamics equation modified with nonlinear elastic forces. Mignolet and Soize [4] showed that the nonlinear elastic forces can be traced back to the elasticity equations, supposing a linear relationship between the Second Piola-Kirchoff stress tensor and the Green strain tensor. Following a Galerkin approach with a basis of functions previously identified, an equation with quadratic and cubic terms describes the dynamics in an approximate way.

Since the nonlinear terms should be quadratic and cubic, most of the ROM approaches up to now have tried to fit the nonlinear coefficients to such polynomials. Muravyov *et al.* [3] suggested enforcing large displacements and obtaining the forces from the FEM solutions. However, the predictions obtained with this approach had limited accuracy and required many linear modes in the basis. McEwan *et al.* [5] proposed to impose large forces in the shape of the linear modes and get the nonlinear displacements from the FEM static solutions. This method proved to be more accurate when applied to structures like shells with constrained boundaries under intense acoustic excitation. Imposing forces instead of displacements allows the nonlinear inplane motion to develop, which usually accompanies large out-of-plane displacements. The method of McEwan *et al.* [5] is called Implicit Condensation (IC).

Later, Hollkamp and Gordon [6] proposed to recover the in-plane displacements from the out-of-plane ones, supposing a quadratic relation between them. The coefficients of the quadratic functions were then fitted from the nonlinear residue of the static training cases. This Implicit Condensation and Expansion (ICE) method allowed a better description of the displacement and stress.

More recently, Ritter *et al.* [7] introduced a new approach, denoted as Enhanced Modal Approach (EnMA), using the modal components of the applied static forces as degrees of freedom. The static results showed good accuracy compared against Nastran reference solutions, using a beam and later a realistic wing box.

In the great majority of the work present in the literature, the geometric nonlinearities are investigated in plate/shell-type structures constrained on all borders. For those structures, the level of displacements that drives geometric nonlinearities is of the order of multiples of the plate/shell thickness and, therefore, the inertia associated to the in-plane motion is not so important, compared to the out-of-plane one. However, for beam-like structures, the displacements are on the order of the structure span (typically over 20% or so of the beam length). At that point, the geometric nonlinear effects will impact the structural inertias and, therefore, the modal mass as well.

2 STRUCTURAL DYNAMICS ROM FORMULATION

2.1 Review of ICE Formulation

Previous developments of structural ROM methodologies are based on equations derived from a Galerkin approach to solve the dynamics in a weak form. For example, Mignolet and Soize [4] used the dynamic equations based on the Second Piola-Kirchoff stress tensor:

$$\frac{\partial\left(F_{ij}S_{jk}\right)}{\partial X_k}+\rho_0 b_i^0=\rho_0\ddot{u}_i \qquad i,j,k=1,2,3 \tag{1}$$

where the tensor $\mathbf{S}$ is the Second Piola-Kirchoff stress tensor, the tensor $\mathbf{F}$ is the deformation gradient tensor, ρ_0 is the mass density in the undeformed structure, and $\mathbf{b^0}$ is the volumetric force, pulled back to the undeformed system.

In order to approximate the solution with the Galerkin approach, a set of basis functions that describes the displacement can be written as

$$u_i\left(\mathbf{x}\right) = \sum_{j=1}^{n} \Phi_{ij}(\mathbf{x}) q_j \tag{2}$$

where $\Phi_{ij}(\mathbf{x})$, which is 2p times differentiable and satisfies all the boundary conditions, represents the component i of the j^{th} basis function, q_j represents the amplitudes and u_i are the components of the displacement of point $\mathbf{x}$ in the reference configuration.

Replacing Eq. (2) in Eq. (1) and making the error orthogonal to the basis functions, Mignolet and Soize [4] shows that a third degree polynomial describes the nonlinear forces in terms of the displacement amplitudes, i.e.,

$$M_{ij}\ddot{q}_j + K^{(1)}_{ij} q_j + K^{(2)}_{ijl} q_j q_l + K^{(3)}_{ijlp} q_j q_l q_p = F_i \tag{3}$$

where the terms M_{ij} are the entries of the reduced mass matrix, F_i is the modal component of the external force, and the terms $K^{(1)}_{ij}$, $K^{(2)}_{ijl}$ and $K^{(3)}_{ijlp}$ are the components of tensors of reduced stiffness. The analytical expression of these terms is related to the displacement basis functions and the constitutive relations for the material, as Mignolet and Soize [4] shows. However, the explicit calculation of these coefficients is not practical for a complex finite element structural model.

In order to apply the Galerkin method above, there are different techniques for the selection of the displacement basis. One of the most common choices is a truncated basis of the linear normal modes of the undeformed structure.

The identification of the nonlinear stiffness coefficients of Eq. (3) is an involving task. Usually, a set of nonlinear static solutions provides a database for the fitting of the coefficients. There are different methods to apply the loads for the generation of the static solutions. One possible approach is to enforce displacements exactly in the shape of the linear modes, exciting amplitudes large enough for the nonlinear effects to appear. Another method applies forces in the shape of the linear modes or combinations of them, e.g.:

$$F = K\left(\alpha\Phi_i + \beta\Phi_j\right) \tag{4}$$

where F is the finite element column matrix of applied loads, K is the linear stiffness matrix of the structure and Φ_i and Φ_j are the columns of generalized displacements corresponding to the modes i and j, while α and β are amplitudes selected to excite the nonlinearities.

Usually, enforcing displacements in the shape of modes may lead to identification problems, especially for cantilevered structures. In fact, as pointed out by Kim *et al.* [8] and Wang *et* *al.* [9], this procedure may even lead to stability problems for the resulting ROMs. The selected approach for this paper is similar to the ICE method of Hollkamp and Gordon [6], which applies forces in the shape of linear modes and uses dual modes afterwards for the recovery of displacements.

Eq. (3) would be exact if the Galerkin approach used a complete basis of displacements. Since a few degrees-of-freedom should represent the displacement, the selected basis functions may not be enough to represent arbitrarily high displacements of cantilevered structures. For example, a few linear modes will not show the shortening of the span-wise projection of a wing. However, it is possible to use a static condensation method, like in McEwan *et al.* [5], and approximate Eq. (3) to take into account this kind of displacement that accompanies the linear modes. In the static condensation approach, the part of displacement which is not spanned by the selected basis is assumed as a higher-order function of the degrees-of-freedom q_i. As Kim *et al.* [8] showed, some approximations lead to quadratic functions that represent this displacement orthogonal to the basis. The main components of this space are usually extracted using a Proper Orthogonal Decomposition (POD).

In the context of the finite element method, the column matrix of generalized displacements X^i of each training case i is decomposed onto the basis of selected modes Φ, i.e.,

$$q^i = \Phi^T M X^i \tag{5}$$

where M is the mass matrix of the structure. Then, it is possible to get the nonlinear residue of displacement for each training case i, subtracting the components along the selected basis Φ, like in the following equation:

$$R_i = X^i - \Phi q^i \tag{6}$$

Stacking the residue for all N training cases, a snapshot matrix R is obtained. The eigenvectors corresponding to the highest eigenvalues of the matrix RR^T constitute the dual modes Ψ:

$$R = [R_1 \; R_2 \; ... \; R_N] \tag{7}$$

$$\Psi = eig(RR^T) \tag{8}$$

In practice, the dual modes will contain the span-wise shortening and other displacements which are geometrically related to the large motion. In order to simplify the dynamic equations, some methods apply a Gram-Schmidt orthogonalization to the dual modes. The number of dual modes to be selected depends on quality of the displacement representation. Some previous studies (e.g., Wang *et al.* [9]) have achieved best results using a basis of dual modes with size similar to the linear basis.

After the selection of the dual modes, displacements are represented using both the primary basis Φ and the dual modes Ψ, like in the following:

$$u = \Phi q + \Psi r \tag{9}$$

where r are the amplitudes of the dual modes. From the hypothesis of the static condensation procedure [8], the lowest-order approximation for the amplitudes of the dual modes is a quadratic dependence on the components along the selected basis, q_i. Hollkamp and Gordon [6] also used this approximation in the original description of the ICE method. Consider:

$$r_i = C_{ij} q_i q_j \quad \text{for} \quad i, j = 1, ..., n \tag{10}$$

where r_i is the component of displacement along the dual mode Ψ_i and C_{ij} are the coefficients of the quadratic terms with all the n components along the linear basis. The identification of the C_{ij} terms uses the same set of nonlinear static solutions that determined the dual modes.

Expressing the displacements with an augmented basis of dual modes was the novelty that the ICE method introduced, relative to the previous IC method of McEwan *et al.* [5]. This expansion of the displacement does not enter into the traditional reduced order structural dynamics, Eq. (3), but it is important for the correct recovery of displacements and stresses. For the structural dynamics formulation to be complete, it is necessary to identify the nonlinear stiffness terms $K^{(2)}_{ijl}$ and $K^{(3)}_{ijlp}$. Again, the dataset of nonlinear static solutions serves for the identification purposes. A least-squares fitting determines the quadratic and cubic coefficients from the nonlinear modal forces, i.e.,

$$\left.\begin{array}{r} K^{(2)}_{ijl} q^1_j q^1_l + K^{(3)}_{ijlp} q^1_j q^1_l q^1_p = F^1_i - K^{(1)}_{ij} q^1_j \\ K^{(2)}_{ijl} q^2_j q^2_l + K^{(3)}_{ijlp} q^2_j q^2_l q^2_p = F^2_i - K^{(1)}_{ij} q^2_j \\ \cdots \\ K^{(2)}_{ijl} q^N_j q^N_l + K^{(3)}_{ijlp} q^N_j q^N_l q^N_p = F^N_i - K^{(1)}_{ij} q^N_j \end{array}\right\} \rightarrow K^{(2)}_{ijl} \quad K^{(3)}_{ijlp} \tag{11}$$

In Eq. (11), the linear least-squares determines the components of the tensors $\mathbf{K}^2$ and $\mathbf{K}^3$, in a general sense. However, there are some symmetries in those tensors from their own definition using the Galerkin approach and from the particular geometry under consideration. Using the static solutions, actually it is only possible to identify the coefficients of the polynomial terms $q_j q_l$ and $q_j q_l q_p$, without difference regarding the order of the factors. For example, instead of identifying K_{12} and K_{21}, it is possible to identify $K_{12} + K_{21}$, which is the coefficient of the binomial $q_1 q_2$ in Eq. (11). That is enough to compose all the nonlinear force of Eq. (3).

For certain structures with symmetries like flat beams, some simplifications are valid, like the assumption of no quadratic stiffness terms. However, there are risks of errors in the simplifications. Hollkamp and Gordon [6] used no simplifications for the polynomials in their original work.

Finally, the reduced order structural dynamics equations for the original ICE method uses only degrees of freedom related to the linear basis initially selected, but quadratic and cubic nonlinear elastic terms implicitly take into consideration a more complex field of displacements. The hypothesis is that the components of the displacement along an initially selected basis Φ determine statically the components along a basis of dual modes Ψ through a quadratic relation.

2.2 Proposed Improvements for the ICE Formulation

2.2.1 Kinetic Energy Enhancement

For shell-like structures constrained at all borders, the nonlinear effects take place when the transverse displacements are in the order of the thickness. In these cases, the membrane effects play an important role in the stiffness, but their contribution to the inertia forces is relatively small. For this reason, the reduced mass matrix M in Eq. (3) is assumed equal to the linear solution's one. For cantilevered structures like high-aspect ratio wings, nonlinear effects on the stiffness only make difference when the tip displacements are of the order of the span, and usually the motion along the dual basis Ψ makes a significant contribution to the inertia forces. To account for this effect properly, one can go back to the Euler-Lagrange equations, i.e.,

$$\frac{d}{dt}\left(\frac{\partial T}{\partial \dot{q}_i}\right) - \frac{\partial T}{\partial q_i} + \frac{\partial U}{\partial q_i} = F^T \frac{\partial u}{\partial q_i} \quad \text{for} \quad i = 1, ..., n \tag{12}$$

where T is the kinetic energy, q_i and $\dot{q}_i$ are the degrees of freedom and their time derivatives, respectively, u is the column matrix of displacements or rotations related to each degree of freedom of the finite element model, F is the column matrix with the external forces or moments applied at each of those degrees of freedom, and the potential energy of the structure U is equal to the strain energy. There is no damping, initially.

2.2.2 Generalization of the ROM Formulation

This work proposes to use the Euler-Lagrange equations as a starting point for the structural ROMs. It has the advantage of generalizing the order reduction methodologies. Since it is based on the kinetic and potential energies, the dual modes will be automatically included in the kinetic energy, via its displacement relation. Besides that, the potential energy may be any function of the generalized coordinates, and will not be restricted to polynomial functions.

Looking at the Euler-Lagrange equations (Eq. 12), three main characteristics need further definition:

- Choice of the degrees of freedom;
- Relationship between the strain energy and the degrees of freedom;
- Relationship between the kinetic energy and the degrees of freedom with its time derivatives.

Using the Euler-Lagrange equations, the displacements are not the only option for the degrees of freedom anymore. Another possibility is to use the internal force to characterize the elastic state of the structure, for example. This approach was already explored by Ritter *et al.* [7], where a reduced order structural model used only the components of the applied force to characterize the potential energy of the structure based on nonlinear static solutions. This method was called Enhanced Modal Approach (EnMA) and its particular implementation also used an expansion process for the displacements, just like the ICE method. However, instead of a quadratic relationship for the dual modes, EnMA uses a fourth-degree polynomial with fitted coefficients for all the dof of the structure. It expresses the displacement as a function of the modal components of the elastic force, which in the static case is equal to the applied force.

In order to illustrate the different choices for the three main aspects of the structural reduced order modeling, Table 1 presents the choices of the ICE and EnMA methods regarding those characteristics.

	ICE	EnMA
Degrees of freedom	Modal components of displacements	Modal components of static force
Displacements function	Quadratic function of the degrees of freedom	4th degree polynomial of the degrees of freedom
Strain energy function	4th degree polynomial of the degrees of freedom	4th degree polynomial of the degrees of freedom

Table 1: Comparison of the ICE and the EnMA methods regarding the main characteristics of ROM.

The functions relating both the displacements and the strain energy with the degrees of freedom are typically polynomials, but could be any nonlinear function. In this paper, two different structures illustrate the reduced order methodology, comparing results against Nastran solutions. The methods for both structures use second-degree polynomials to model the dual modes components, but they use different functions for the potential energy. One solution uses a fourth-degree polynomial to represent the potential energy and the other one uses a neural network to fit directly the derivatives of the potential energy, which are the nonlinear forces.

One of the important ideas of this paper is the flexibility in the choices of the structural reduced order models. Surely, the Galerkin approach and Eq. (3) give a backbone for the developments of the reduced models. However, the static condensation implies that Eq. (3) is not exact anymore, and other fitting functions may perform better in large displacements. The fitting is not an easy process, and will never be exact, but if it captures the basic nonlinearities involved, that may be enough for aeroelastic analysis and controls design.

3 IMPLEMENTATION

In order to approximate a structural solution with a reduced order model, it is necessary to first fit coefficients for the displacement and potential energy or nonlinear force functions. Then, Euler-Lagrange equations are integrated in time with an appropriate nonlinear solver. This section explains the process and some details of the particular implementation of this paper, summarized in Fig. (1).

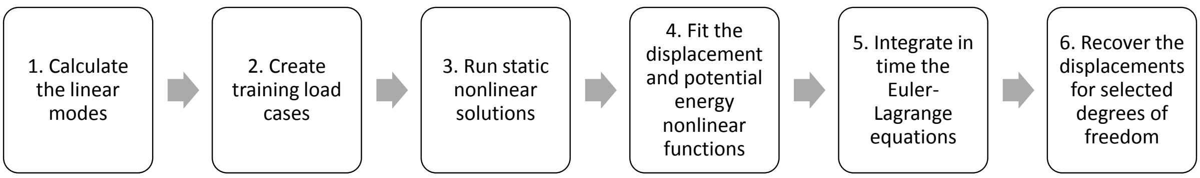

Figure 1: Process of the structural reduced oder model creation and solution.

3.1 Training Load Cases

In order to capture the nonlinearities of the potential energy and the nonlinear displacements, it is necessary to train the fitting functions with loading conditions that excite these nonlinearities. At the same time, it is desirable to cover conditions similar to the expected simulations to be performed. The choice of the training cases is the second step of the process shown in Fig. (1).

Unfortunately, as the degrees of freedom grow, it becomes harder to keep a reasonable density of samples over the domain of expected solutions. One alternative to reduce this problem is to prioritize some modes which are more important, like the first bending modes. For the examples shown in this paper, the training sets are composed of nonlinear solutions for excitations in the shape of each selected linear mode alone and excitations composed of the first mode and each of the other modes, observing Eq. (4). These combinations of forces use a range of different amplitude ratios for the modes.

Obtaining static solutions for the training load cases is the step 3 of the process. In this case, using a set of increasing amplitudes for a given combination of forces will speed up the calculations, since the solutions are obtained sequentially. It was checked that a Nastran SOL 400 static simulation matches the converged state of an equivalent dynamic case with damping.

3.2 Choosing the Number of Nonlinear Coefficients

One of the main issues of the structural reduced order modeling is the choice of the nonlinear functions fitted in the step 4 of the process. In general, for the accuracy of the fitting to be high, the nonlinear functions should have enough flexibility to approximate the training points. However, if the number of parameters to be fitted is large, overfitting may happen. Usually, the complete polynomials will have a large number of parameters. For a system with n degrees of freedom, the number of polynomial terms of degree r can be determined from:

$$n_r = \binom{n+r-1}{r} \tag{13}$$

With only 9 degrees of freedom, for example, there are 495 polynomial terms of fourth degree. In order to reduce the number of terms, there are different approaches to select the most important terms. The work of McEwan [10] summarizes some methods. For the results of this work, the elimination of the less important polynomial terms follows the one-step regularization procedure given in Sjöberg [11]. This procedure uses the Hessian matrix of the regularized error to classify the most important terms by their order of importance.

3.3 Equations and Time-integration Scheme

This subsection gives an example of the equations for the ICE approach. This formulation shows the detailed development of the kinetic energy derivatives, accounting for the effects of the dual modes, which are important for cantilevered structures. Also, the development here follows a matrix formulation for fast solutions.

3.3.1 Kinetic Energy and its Derivatives

In the ICE formulation, the displacement depends on the degrees of freedom q and on the amplitudes of the dual modes r, like in Eq. (9). The column matrix r is composed of quadratic combinations of the terms q, according to Eq. (10). So, the velocity may be expressed as:

$$\dot{u} = \Phi\dot{q} + \Psi\frac{\partial r}{\partial q}\dot{q} \tag{14}$$

where the matrix of derivatives of the quadratic terms with respect to the degrees of freedom is given by:

$$\frac{\partial r}{\partial q} = \begin{bmatrix} \frac{\partial r_1}{\partial q_1} & \frac{\partial r_1}{\partial q_2} & \frac{\partial r_1}{\partial q_3} & \cdots & \frac{\partial r_1}{\partial q_n} \\ \frac{\partial r_2}{\partial q_1} & \frac{\partial r_2}{\partial q_2} & \frac{\partial r_2}{\partial q_3} & \cdots & \frac{\partial r_2}{\partial q_n} \\ \vdots & \vdots & \vdots & \ddots & \vdots \\ \frac{\partial r_s}{\partial q_1} & \frac{\partial r_s}{\partial q_2} & \frac{\partial r_s}{\partial q_3} & \cdots & \frac{\partial r_s}{\partial q_n} \end{bmatrix} \tag{15}$$

In the velocity equation, $\dot{u}$ is the column matrix of time derivatives of all the degrees of freedom of the FEM, while $\dot{q}$ is the time derivative of the degrees of freedom of the structural reduced order model. It is assumed that the column matrix of quadratic terms r has s components and the number of degrees of freedom of the ROM is n.

The kinetic energy is defined using the velocity and the mass matrix of the FEM. This mass matrix is assumed constant, which is generally a good approximation even for very flexible structures, according to Pai [12]. The general expression for the kinetic energy can be written as:

$$T = \frac{1}{2}\dot{u}^T M \dot{u} = \frac{1}{2}\left(\dot{q}^T\Phi^T + \dot{q}^T\frac{\partial r}{\partial q}^T\Psi^T\right) M \left(\Phi\dot{q} + \Psi\frac{\partial r}{\partial q}\dot{q}\right) \tag{16}$$

and defining:

$$\Phi^T M \Psi = M_X \tag{17}$$

$$\Psi^T M \Psi = M_\Psi \tag{18}$$

leads to:

$$T = \frac{1}{2}\dot{q}^T \underbrace{\left(I_n + 2M_X\frac{\partial r}{\partial q} + \frac{\partial r}{\partial q}^T M_\Psi \frac{\partial r}{\partial q}\right)}_{M'} \dot{q} \tag{19}$$

Using the notations defined in Eqs. (17) and (18), the kinetic energy can be simplified to a format with a reduced mass matrix M', in Eq. (19), where I_n is an identity matrix of size $n \times n$.

For the Euler-Lagrange equations, it is necessary to take the time derivative of the kinetic energy, i.e.,

$$\frac{d}{dt}\left(\frac{\partial T}{\partial \dot{q}_i}\right) = \frac{dM'}{dt}\dot{q} + M'\ddot{q} \tag{20}$$

and:

$$\frac{dM'}{dt} = 2M_X \frac{d}{dt}\frac{\partial r}{\partial q} + \left(\frac{d}{dt}\frac{\partial r}{\partial q}\right)^T M_\Psi \frac{\partial r}{\partial q} + \frac{\partial r}{\partial q}^T M_\Psi \frac{d}{dt}\frac{\partial r}{\partial q} \tag{21}$$

The time derivative of the reduced mass matrix involves the matrix $\left(\frac{\partial r}{\partial q}\right)$ that comes from a reshape process using the matrix $\left(\frac{\partial^2 r}{\partial q^2}\right)$, which is the row stacking of derivative matrices, i.e.,

$$\frac{d}{dt}\frac{\partial r}{\partial q} = \left[\left(\frac{\partial^2 r}{\partial q^2}\right)_{sn\times n} \dot{q}\right]_{s\times n} \quad \text{where} \quad \left(\frac{\partial^2 r}{\partial q^2}\right)_{sn\times n} = \begin{bmatrix} \frac{\partial^2 r}{\partial q_1 \partial q} \\ \frac{\partial^2 r}{\partial q_2 \partial q} \\ \vdots \\ \frac{\partial^2 r}{\partial q_n \partial q} \end{bmatrix} \tag{22}$$

The sub-indexes in Eq. (22) indicate the size of the matrices. The reshape observes the order of the elements along the columns. So, the reshape of Eq. (22) from a column matrix of sn elements to a matrix of size $s \times n$ lays the elements successively along the columns of s rows each. This technique avoids the use of multi-dimensional matrices.

Another term of the Euler-Lagrange equations which is related to the kinetic energy is its derivative with respect to the degrees of freedom q. In matrix form, and resorting again to the reshape technique, this derivative is expressed by:

$$\frac{\partial T}{\partial q} = \left[\dot{q}^T \left(M_X + \frac{\partial r}{\partial q}^T M_\Psi\right)\left(\frac{\partial^2 r}{\partial q^2}\right)_{s\times n^2}\right]^T_{n\times n} \dot{q} \tag{23}$$

where:

$$\left(\frac{\partial^2 r}{\partial q^2}\right)_{s\times n^2} = \left[\frac{\partial^2 r}{\partial q_1 \partial q} \quad \frac{\partial^2 r}{\partial q_2 \partial q} \cdots \frac{\partial^2 r}{\partial q_n \partial q}\right] \tag{24}$$

3.3.2 Elastic and External Forces

The elastic forces originate from the derivatives of the potential energy with respect to the degrees of freedom. A general way to express the potential energy is given by:

$$U = \frac{1}{2}q^T \Lambda q + U_{nl}(q) \tag{25}$$

where U_{nl} is a nonlinear function of the degrees of freedom q. If the primary basis is a truncated set of linear modes, the matrix Λ is a diagonal matrix of its eigenvalues. The elastic force in matrix form is composed of both a linear and a nonlinear term, and is given by:

$$\frac{\partial U}{\partial q} = \Lambda q + \frac{\partial U_{nl}}{\partial q} \tag{26}$$

The right-hand side of Euler-Lagrange equations, Eq. (12), contains the contribution of the external forces F. Taking the derivative of the displacement equation, Eq. (9), yields:

$$f \equiv \frac{\partial u}{\partial q}^T F = \left(\Phi + \Psi \frac{\partial r}{\partial q} \right)^T F \tag{27}$$

which shows the effects of the external forces in both the directions of primary basis and dual modes. It is important to consider that the external forces may excite directly the dual modes, but the response of the structure will always involve the primary degrees of freedom selected. With this approach, the effects of follower forces are properly accounted for.

3.3.3 Euler-Lagrange Equations in Matrix Form

With the derivatives of the kinetic and potential energies and the work of external forces, finally the Euler-Lagrange equations in matrix form can be written as:

$$\begin{aligned}
&\left(I_n + 2M_X \frac{\partial r}{\partial q} + \frac{\partial r}{\partial q}^T M_\Psi \frac{\partial r}{\partial q} \right) \ddot{q} + \\
&\left[2M_X \frac{d}{dt}\frac{\partial r}{\partial q} + \frac{d}{dt}\frac{\partial r}{\partial q}^T M_\Psi \frac{\partial r}{\partial q} + \frac{\partial r}{\partial q}^T M_\Psi \frac{d}{dt}\frac{\partial r}{\partial q} - \left[\dot{q}^T \left(M_X + \frac{\partial r}{\partial q}^T M_\Psi \right) \left(\frac{\partial^2 r}{\partial q^2} \right)_{t\times n^2} \right]^T_{n\times n} \right] \dot{q} \\
&= \left(\Phi + \Psi \frac{\partial r}{\partial q} \right)^T F - \Lambda q - \frac{\partial U_{nl}}{\partial q}
\end{aligned} \tag{28}$$

The expression above does not include the contribution of the damping. In order to include it, the simple linear term $\beta\Lambda\dot{q}$ may be added to its left-hand side. The parameter β indicates the value of the damping. Experience has shown that the linear damping is enough to match the Nastran results, even for large displacements. In fact, the dual modes do not contribute to the damping, which is related to the rate of strain energy. It is possible to refine the damping using the nonlinear potential energy, but all tests have revealed that this correction is negligible.

3.3.4 Time Integration Scheme

Time integration of the equations is the step 5 of the process in Fig. (1). The complete Euler-Lagrange equations show that the dynamics involve q, $\dot{q}$ and $\ddot{q}$. Time integration schemes for stiff equations may solve efficiently this second-order system of ODEs. For this particular work, the MATLAB function ode15s solves the equivalent first-order system as:

$$M(t,Q)\dot{Q} = R(t,Q) \;\text{ where }\; Q = \begin{Bmatrix} q \\ \dot{q} \end{Bmatrix} \tag{29}$$

where the mass matrix $M(t,Q)$ and the right-hand side matrix $R(t,Q)$ derive from the Euler-Lagrange equations.

The time-integration scheme for all the results in this paper is the ode15s function of MATLAB. More details about this approach can be found in Shampine and Reichelt [13]. This method is an implicit variable-order integrator with adaptive time step. It is efficient for stiff systems, but is useful also for non-stiff ones, since the Jacobian of the right-hand side of Eq. (29) is evaluated only when needed.

3.4 Recovery of Displacements

Finally, the recovery of a selected set of degrees of freedom is the last step in the process of Fig. (1). The solution history provides the degrees of freedom and its derivatives at all simulation times. Particular reference node displacements may be recovered after the time integration using:

$$X_{ref} = \Phi_{ref} q + \Psi_{ref} r(q) \tag{30}$$

where the matrix of linear modes Φ_{ref} and the matrix of dual modes Ψ_{ref} include only the selected degrees of freedom. As a practical consideration, it is important to notice that in the previous equations of the modal formulation, the matrices Φ and Ψ represent the active degrees of freedom, which may be requested from the FEM modal solution. The entries of Φ_{ref} and Ψ_{ref} are related to the linear and dual modes, but are not necessarily contained in the active set.

4 NUMERICAL RESULTS

In order to evaluate the accuracy of the proposed reduced order methodology, this work compares mainly the dynamic results for displacements in the time-domain. Two structures are used: a 16-m straight beam illustrative of a high-aspect ratio wing and a wing box representative of the Bristol Ultra Green (BUG) concept.

All the trainings of nonlinear fittings used Nastran SOL 400 static solutions. For this reason, Nastran SOL 400 dynamic solutions are assumed as the reference for the comparisons. From benchmarks of beam solutions developed with other researchers as part of an internal effort, it is believed that Nastran is able to reproduce accurately the nonlinear dynamic behavior, if the time integration uses a small time step.

For the 16-m beam, particularly, results from the multibody dynamics simulation software ADAMS are plotted along with the Nastran and ROM solutions. ADAMS has a built-in implicit nonlinear finite element solver, and its results are useful to evaluate the accuracy of the ROM method when compared to different nonlinear results.

All nonlinear solutions are also compared against their linear counterparts. An integration in Matlab using the same linear modes of the ROM solution provides linear results. In the case of follower forces, like for the 16-m beam examples, the linear solution uses the local orientation of the structure to apply the follower loads.

4.1 16-m Straight Beam

The 16-m straight beam represents the semi-span of a high-aspect ratio wing of a High Altitude Long Endurance (HALE) aircraft [14].

The beam model is the one developed in Ritter *et al.* [7], and it is shown in Fig. (2).

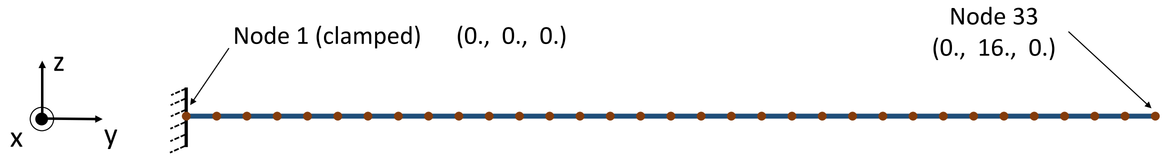

Figure 2: 16-m straight beam used for displacement comparisons.

In this paper, all the static solutions for the training of the reduced order model use the Nastran FEM package. For the beam model, a total of 32 CBEAM elements are used. The area moment of inertia decreases from root to tip, and there are concentrated masses at all nodes.

For this example, the analysis is focused on the displacements along the y-z plane, which is the vertical plane. There is no loading in the x-directions nor torsion. Also, the coupling terms of stiffness and inertia matrices are all zero.

The linear basis Φ consists of 6 bending modes, with frequencies from 0.59 Hz to 32 Hz. Using a basis of 6 modes allows a modal effective mass of 90% in the vertical direction z. A set of 10 dual modes complements the linear basis to represent displacements along the vertical plane. The dual modes, calculated from the nonlinear residue of static solutions like in Eq. (8), allow to describe the shortening of the beam's horizontal projection.

Training the beam, the static cases covered all the single mode excitations and combinations of forces in the shapes of two different modes. The amplitudes are high enough to excite the nonlinearities and represent large displacements. For each excited linear mode, the degree of nonlinearity is measured according to the ratio between the nonlinear and the linear displacements for a given degree of freedom, like the tip vertical displacement. There are indications in the previous works by Kuether *et al.* [15] that this ratio should be around 0.8 and 0.95 for hardening nonlinearities, which is the case for a beam. However, that indicator is only valid for shell-type structures with all sides constrained. For cantilevered beams, smaller ratios as 0.6 have shown good results. Actually, the amplitudes of the training loads should be adequate to the load cases of interest. If the displacements obtained in the simulations are higher or close to the training limits, it is necessary to train again the reduced order model.

A total of 2,240 Nastran nonlinear static results compose the training set of solutions. The time for this training is around 5 minutes in a Xeon E3 processor.

If the fitting for the potential energy is polynomial, a regularization process leads to the identification of 74 polynomial terms of fourth-degree that represent the nonlinear potential energy. If the neural network is the choice for the model fitting, a model with two hidden layers and 25 parameters is enough for a good generalization of the predictions.

Two load cases are analyzed:

- Load Case 1 (LC1): 1-kN follower force applied at the tip of the beam in the vertical direction as a step input at the initial time, with no damping for the structure;
- Load Case 2 (LC2): follower sinusoidal force of amplitude 2.0 kN and frequency 0.25 Hz applied at the tip of the beam in the vertical direction, starting at the initial time, with no damping for the structure.

Figure 3 shows the tip vertical displacements for Load Case 1, together with the evolution of error relative to the Nastran solution. Initially, the linear solution is an accurate approximation. As time evolves, a phase error is developed, but the ICE solution remains close to the Nastran reference curve. This shows a good agreement in terms of the frequency of the nonlinear solution. The ADAMS solution remains close to the Nastran one. However, this case shows that the discrepancy between ICE and Nastran (Fig. 3) is similar to the discrepancies between those two reference solvers.

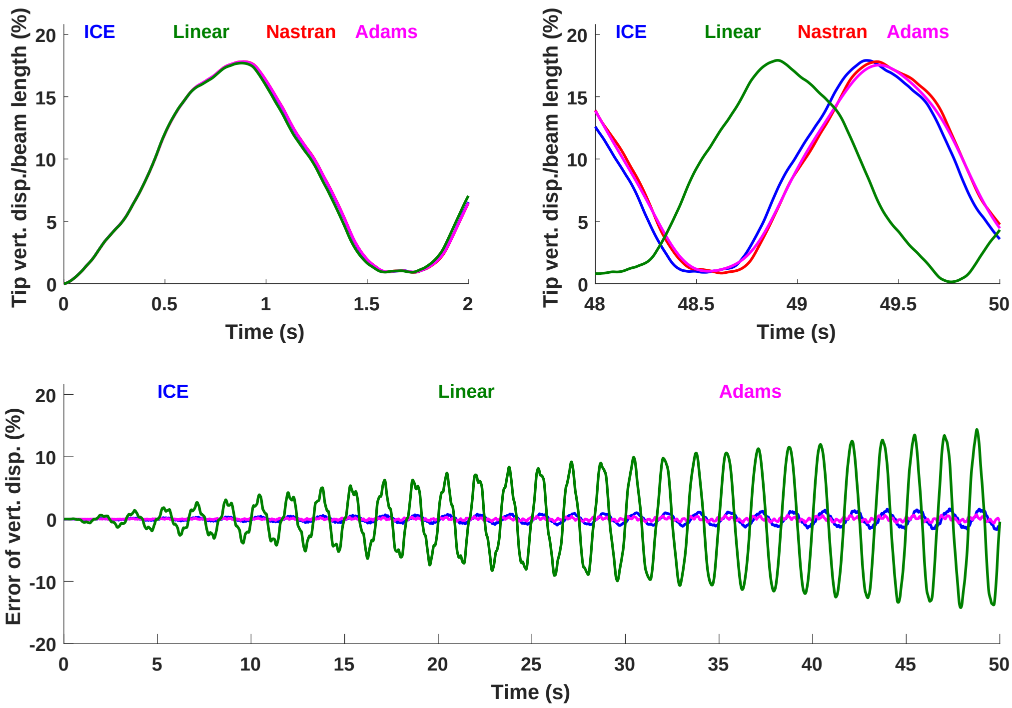

Figure 3: Tip vertical displacements of the 16-m beam for Load Case 1.

One of the main advantages of the ICE solution is the possibility to model displacements not included in the linear basis. For the 16-m beam, Fig. 4 presents the comparison of span-wise displacements as the beam deflects. The displacement comparison on the left plot shows that the accumulated errors in 50 s of simulation are small, and the error plot on the right reveals that the error of the ICE in the span-wise direction is comparable to the differences between the Nastran and ADAMS solutions. The linear solution is not capable of capturing this shortening effect.

Loading the beam with a sinusoidal force as defined in Load Case 2, it is possible to see more remarkable differences between the linear and the nonlinear solutions since the displacements are higher. Figure 5 compares the tip vertical displacement according to the linear, ICE, ADAMS and Nastran solutions. ICE is able to reproduce the behavior of the Nastran solution up to deflections of 30%.

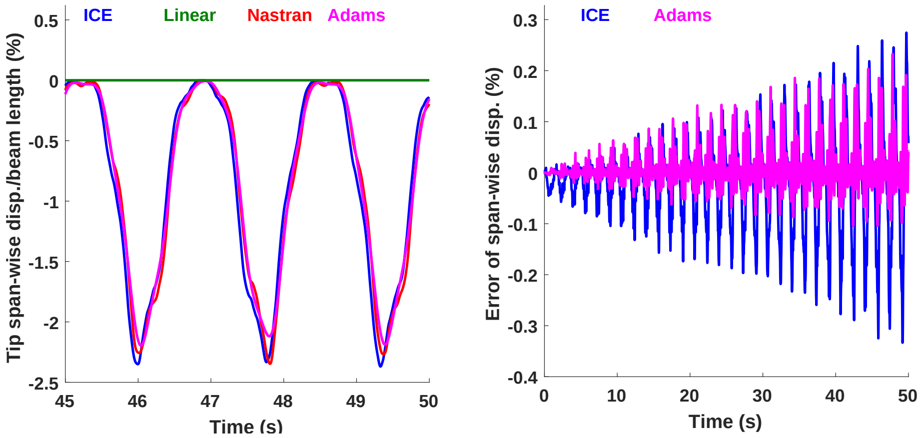

Figure 4: Span-wise displacements of the 16-m beam for Load Case 1.

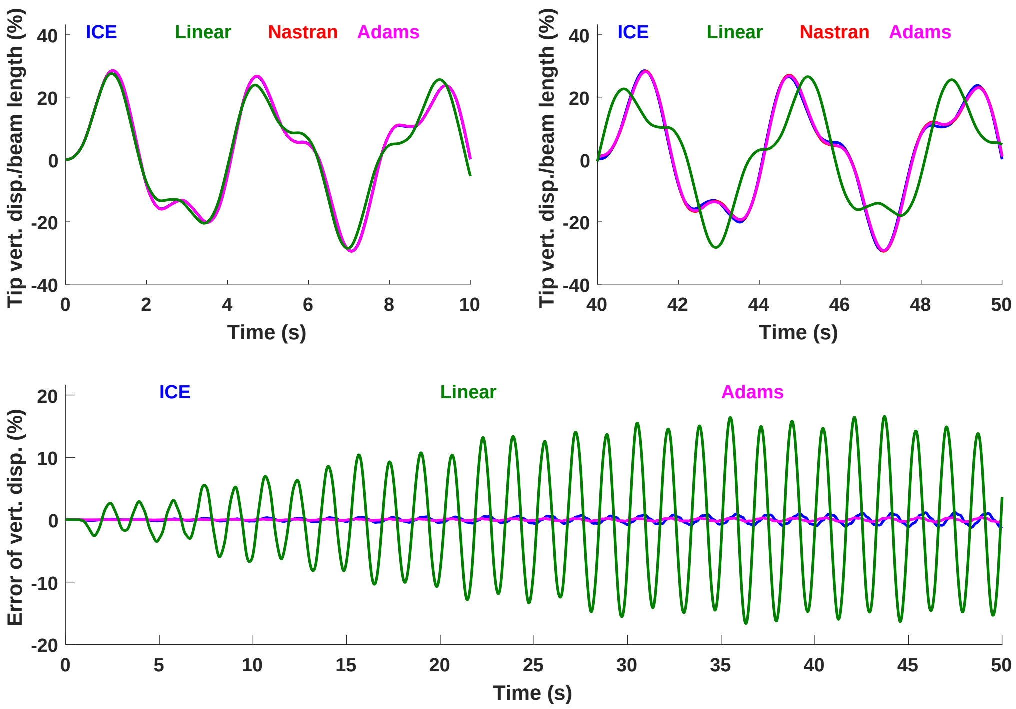

Figure 5: Vertical displacements of the 16-m beam for Load Case 2.

4.2 BUG Wing Box

The second example features a more complex structure. It is a realistic wing box FEM model comprised of shells and beams, with a total of 48,136 degrees of freedom. This model was developed by the University of Bristol to represent the wing of the Bristol Ultra Green concept. Figure 6 shows the FEM model. This wing is suited for the analysis because it has a large aspect ratio, close to 19 for the full wing. Also, this structure is able to undergo large displacements without serious instability problems. The BUG wing is constrained with wing-fuselage boundary conditions, and the particular composite layup of this model makes it coupled between bending and torsion.

Since it is a more complex model than the 16-m beam, more degrees of freedom are needed to represent its dynamics properly. In this case, nine degrees of freedom were selected as the projections of displacement onto the first nine linear modes.

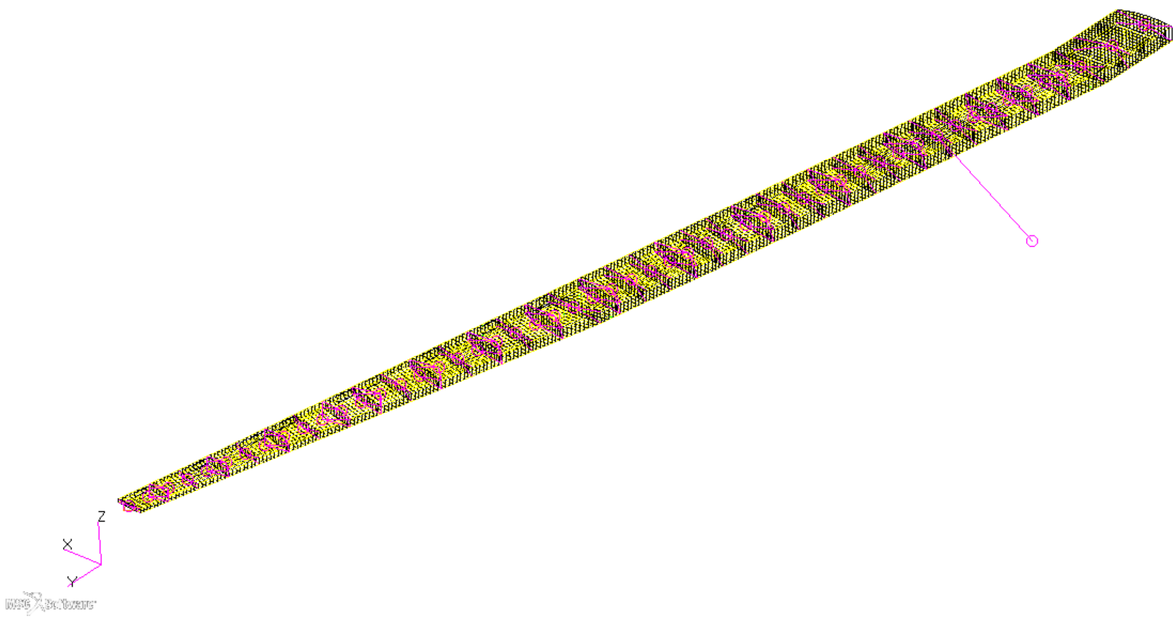

Figure 6: Bristol Ultra Green (BUG) wing Nastran model.

The set of the first 9 linear modes include four out-of-plane bending modes, two in-plane modes and the first torsion mode, with frequencies up to 15 Hz.

Training the ICE model involved nonlinear static solutions with forces in the shape of the linear modes, as in the case of the 16-m beam. In total, 3,960 solutions composed the training base. Using a Xeon E3 processor, it takes 7 hours to simulate these cases using SOL 400.

For the nonlinear force fitting, solutions with both polynomials and neural networks were developed. The comparisons showed that a better fitting could be achieved with a neural network function to model the nonlinear force as a function of the degrees of freedom. In this case, a neural network model with two hidden layers containing four neurons in the first layer and two neurons in the second one presented the best performance. Training it with the Levenberg-Marquadt method implemented in the Matlab Neural Network Toolbox takes less than 2 minutes.

The BUG wing results are compared here using a step loading in the shape of the first mode, which is the out-of-plane bending. There is a structural damping of 0.5%. Using this kind of loading, the structure can undergo large displacements and still have a converged Nastran solution for comparison.

Figure 7 shows the comparison of displacements of the wing tip at the center of the wing box. In this case, there is motion in all three dimensions, and the ICE solution provides a good estimate for the nonlinear displacement in all directions. For this kind of loading, which is similar to the cases of the training base, the similarity between the ICE and the complete Nastran solution is so good that no visual difference is noticed in the plots.

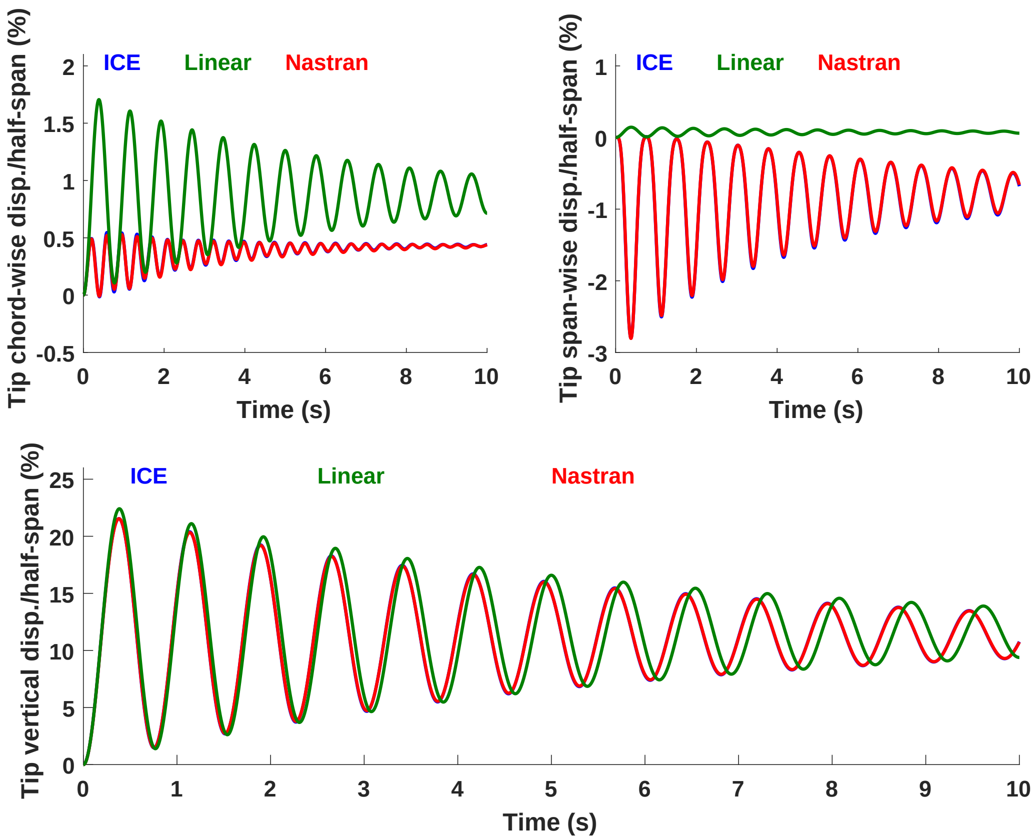

Figure 7: Tip displacements of the BUG wing model with a step loading in the shape of the first vertical bending mode.

Ten dual modes complemented the basis of 9 linear modes. The amplitudes of the dual modes were fitted with all quadratic combinations of the 9 degrees of freedom.

As the model grows in size, the benefits of the ROM solutions are greater. In the case of the BUG wing, for example, the time to run the complete model in Nastran for 10 s of simulation was of 8h 10m with a Xeon E3 processor. The same simulation with the ICE method took 11 s with a script written in MATLAB. So, for the case shown in Fig. 7, the training time of the ROM model was shorter than the time to run the complete model for 10 s. Such quick ROM simulations open the opportunity to use the structural ROMs for real-time applications.

Not all conditions may be suitable to the ICE modeling yet. A caveat of this model is that the loading should be close to the training cases. If the load is higher than the training set, it is possible that the predictions of the nonlinear displacements will be worse than the simple linear solution. In this case, for example, if one uses a loading very different from the training case, nine degrees of freedom is not enough to have a good matching.

Finally, it became clear during the evaluation of the BUG wing that sometimes it is hard to achieve convergence with the direct Nastran SOL 400 dynamic solution, which may be caused by problems with local instabilities in high displacement conditions. In those cases, the ROM solutions were still able to easily and quickly achieve convergence.

5 CONCLUDING REMARKS

Structural reduced order models were described from the point of view of Euler-Lagrange equations. In this context, a chosen set of degrees of freedom should be used to represent the nonlinear strain energy and the nonlinear displacements using fitted functions. The formulation with this approach was described, leading to the dynamic equations in terms of a few degrees of freedom. This approach allows an extension of modal solutions to geometrically nonlinear conditions.

The contributions of this paper are the inclusion of the nonlinear displacements in the dynamics of reduced order models, correcting the inertia terms, and the generalization of structural ROMs into a framework based on the choice of degrees of freedom and fitted models for strain energy and displacements.

Two different structures were analyzed using the ROM methodology of Implicit Condensation and Expansion (ICE): a 16-m straight beam and a realistic wing box model. Plots of tip displacements with time showed that this methodology is able to predict large displacements accurately if the functions of nonlinear strain energy and displacement are representative of the structure.

There are many challenges yet for a general description of large displacements with a few degrees of freedom. This work used polynomials and neural networks to fit the nonlinear force, and quadratic polynomials for the nonlinear displacements. However, it was not possible to determine a general fitting function and a sampling method suitable for complex structures under a wide variety of loading conditions.

ACKNOWLEDGMENTS

This work is supported by Airbus Americas Inc., with David Hills as the Airbus Project Leader. Technical discussions with him are greatly appreciated. The routines for ROM training were developed in part by Markus Ritter (DLR), and his help with this work is also gratefully acknowledged. Finally, the first author also acknowledges the support of CNPq (Conselho Nacional de Desenvolvimento Científico e Tecnológico, Brazil) and the University of Michigan for his academic scholarship.

6 REFERENCES

[1] Shearer, C. M. and Cesnik, C. E. (2007). Nonlinear flight dynamics of very flexible aircraft. *Journal of Aircraft*, 44(5), 1528–1545.

[2] Thompson, P. M., Klyde, D. H., Farhat, C., and Harris, C. (2007). Aeroservoelastic predictive analysis capability. In *AIAA Atmospheric Flight Mechanics Conference and Exhibit, Guidance, Navigation, and Control and Co-located Conferences*. Hilton Head, South Carolina, 20-23 August 2007. AIAA 2007-6716, 10.2514/6.2007-6716.

[3] Muravyov, A. A., Turner, T. L., Robinson, J. H., and Rizzi, S. A. (1999). A new stochastic equivalent linearization implementation for prediction of geometrically nonlinear vibrations. In *40th AIAA/ASME/ASCE/AHS/ASC Structures, Structural Dynamics and Materials Conference*. St. Louis, Missouri, 12-15 April 1999. AIAA-99-1376, 10.2514/6.1999-1376.

[4] Mignolet, M. P. and Soize, C. (2008). Stochastic reduced order models for uncertain geometrically nonlinear dynamical systems. *Computer Methods in Applied Mechanics and Engineering*, 197, 3951–3963.

[5] McEwan, M. I., Wright, J. R., Cooper, J. E., and Leung, A. Y. T. (2001). A combined modal/finite element analysis technique for the dynamic response of a non-linear beam to harmonic excitation. *Journal of Sound and Vibration*, 243(4), 601–624.

[6] Hollkamp, J. J. and Gordon, R. W. (2008). Reduced-order models for nonlinear response prediction: Implicit condensation and expansion. *Journal of Sound and Vibration*, 318(4), 1139–1153.

[7] Ritter, M., Cesnik, C. E., and Krger, W. R. (2015). An enhanced modal approach for large deformation modeling of wing-like structures. In *AIAA Science and Technology Forum and Exposition (SciTech2015), 56th AIAA/ASCE/AHS/ASC Structures, Structural Dynamics, and Materials Conference*. Kissimmee, Florida, 5-9 January 2015. AIAA 2015-0176, 10.2514/6.2015-0176.

[8] Kim, K., Khanna, V., Wang, X. Q., and Mignolet, M. P. (2009). Nonlinear reduced order modeling of flat cantilevered structures. In *50th AIAA/ASME/ASCE/AHS/ASC Structures, Structural Dynamics, and Materials Conference, Structures, Structural Dynamics, and Materials and Co-located Conferences*. Palm Springs, California, 4-7 May 2009. AIAA 2009-2492, 10.2514/6.2009-2492.

[9] Wang, X. Q., Perez, R. A., and Mignolet, M. P. (2013). Nonlinear reduced order modeling of complex wing models. In *54th AIAA/ASME/ASCE/AHS/ASC Structures, Structural Dynamics, and Materials Conference, Structures, Structural Dynamics, and Materials and Co-located Conferences*. Boston, Massachusetts, 8-11 April 2013. AIAA 2013-1520, 10.2514/6.2013-1520.

[10] McEwan, M. I. (2001). *A Combined Modal/Finite Element Technique for the Non-Linear Dynamic Simulation of Aerospace Structures*. Ph.D. thesis, University of Manchester, Manchester.

[11] Sjoberg, J., Zhang, Q., Ljung, L., Benveniste, A., Delyon, B., Glorennec, P., Hjalmarsson, H., and Juditsky, A. (1995). Nonlinear black-box modeling in system identification: a unified overview. *Automatica*, 31(12), 1691–1724.

[12] Pai, P. F. (2007). *Highly Flexible Structures: Modeling, Computation, and Experimentation*. AIAA Education Series. Reston: AIAA.

[13] Shampine, L. F. and Reichelt, M. W. (1997). The matlab ode suite. *SIAM Journal on Scientific Computing*, 18(1), 1–22.

[14] Patil, M. J., Hodges, D. H., and Cesnik, C. E. S. (2001). Nonlinear aeroelasticity and flight dynamics of high-altitude long-endurance aircraft. *Journal of Aircraft*, 38(1), 88–94.

[15] Kuether, R. J., Deaner, B. J., Hollkamp, J. J., and Allen, M. S. (2015). Evaluation of geometrically nonlinear reduced-order models with nonlinear modes. *AIAA Journal*, 53(11), 3273–3285.

COPYRIGHT STATEMENT